

Coherent dynamics of radiatively coupled quantum-well excitons

T. Stroucken, A. Knorr, P. Thomas, and S. W. Koch

*Fachbereich Physik und Wissenschaftliches Zentrum für Materialwissenschaften, Philipps-Universität, Renthof 5,
D-35032 Marburg, Germany*

(Received 28 July 1995)

The optical response of radiatively coupled semiconductor multiple-quantum-well structures is investigated theoretically. It is shown that the transverse optical field leads to a coupling of exciton states within each well which causes a radiative decay and a mixing of excitonic resonances. Simultaneously, the field-induced long-ranged coupling between different wells leads to collective effects that are very sensitive to the detailed geometry of the structure. For a quantum-well spacing equal to an integer multiple of half the optical wavelength inside the medium, it is predicted that the collective effects cause a stimulated decay of electronic excitations that should be observable in either transmission or reflection geometry. On the other hand, in a quarter wavelength structure, the light-induced coupling causes an interwell energy transport and a splitting of the excitonic resonances, that should be observable as quantum beats in the time-resolved transmitted or reflected signal.

I. INTRODUCTION

During the last few years, the dynamics of excitons and excitonic wave packets in semiconductor multiple-quantum-well structures (MQW's) has been studied extensively.¹ However, in most theoretical investigations propagation effects, i.e., the interaction between excitonic resonances mediated by reemitted photons have been ignored, implicitly assuming that in each well the dynamics of the excitonic excitations in the absence of electronic coupling between different wells is independent of the number of quantum wells (QW's) or of the barrier thickness. However, in recent pump-probe experiments on samples containing one, two, and five QW's an initial population decay time increasing with the number of QW's could be observed,² indicating the existence of collective phenomena in MQW's.

From bulk semiconductors, it is known that propagation effects in optically thick samples lead to pulse breakup and polariton beating,³⁻⁸ but can be neglected in optically thin samples. For such situations and for monochromatic excitation under quasistationary conditions the optical absorption, i.e., the ratio of the transmitted and the input intensity, is directly related to the imaginary part of the optical susceptibility, as is the density of photogenerated electron-hole pairs.⁹

Contrary to the homogeneous case, where the conservation of energy and crystal momentum leads to stationary polariton states, electronic excitations in a quantum well can decay radiatively, i.e., by emitting photons.^{10,11} Due to energy and in-plane momentum conservation, reemitted photons can propagate in either the forward or backward direction, giving rise to partial reflections.¹²⁻¹⁶ As a consequence, the ratio of transmitted and input intensity is no longer a measure for the absorbed intensity.¹⁴⁻¹⁶ Since, in turn, the emitted photons interact with all excitonic transitions in each quantum well, the QW's can no longer be treated as indepen-

dent, but are coupled by the light field and collective effects can occur.

In this paper we present a semiclassical theory of radiatively coupled QW's based on the semiconductor Maxwell-Bloch equations (SMBE's). We derive the SMBE's for a classical optical field interacting with regularly spaced QW's. The individual wells are assumed to be sufficiently thin in order to allow us to deal with the electronic problem in the two-dimensional limit. To demonstrate the basic effects of the light-induced intrawell and interwell coupling we evaluate the theory in the linear regime. Within the coherent time domain, we find a sensitive dependence of the results on the detailed geometry of the structure.

II. THE SEMICONDUCTOR MAXWELL-BLOCH EQUATIONS

In this section, we derive the SMBE's governing the interaction between a classical propagating light pulse and the interband polarization in a MQW. The SMBE's combine the wave equation for the optical field and the semiconductor Bloch equations (SBE's) which determine the microscopic interband polarization. The interband polarization is given by the expectation value of the field-induced optical transitions, thus coupling the classical field to the quantum-mechanical dynamics of the system. Generally, the SMBE's constitute a rather complicated set of coupled differential equations. However, we demonstrate that under certain conditions, the classical and quantum-mechanical part can formally be separated, allowing for a formal solution of the wave equation in terms of the microscopic interband polarization.

We use excitonic units $\hbar = m_r = e^2/\epsilon_0 = 1$ throughout the paper, where m_r is the reduced mass of the electron-hole pair and ϵ_0 is the background dielectric constant. The speed of light in the crystal is related to the dielectric constant by $c = c_{\text{vac}}/\sqrt{\epsilon_0} = \sqrt{\epsilon_0}/\alpha$, where α is the fine-structure constant.

A. Maxwell equations for a classical optical field interacting with semiconductor quantum wells

In this section we concentrate on the wave equation, describing the propagation of a classical optical field interacting with a MQW. Experimentally, the solution of Maxwell's equation,

$$\left(\nabla^2 - \frac{1}{c^2} \frac{\partial^2}{\partial t^2}\right) \mathbf{E}(\mathbf{r}, t) = 4\pi \frac{1}{c^2} \frac{\partial^2}{\partial t^2} \mathbf{P}(\mathbf{r}, t) + 4\pi \frac{1}{c} \frac{\partial}{\partial t} \mathbf{j}(\mathbf{r}, t) + 4\pi \nabla[\rho(\mathbf{r}, t) - \nabla \cdot \mathbf{P}(\mathbf{r}, t)], \quad (1)$$

for the classical radiation field is detected after propagating through the interaction region. From the measured absorption, transmission, or reflection the optical response of the semiconductor, i.e., the field-induced macroscopic charge, current, and interband polarization density, ρ , \mathbf{j} , and \mathbf{P} , must be deduced. In an inhomogeneous structure like a MQW, the induced macroscopic charge and current density, as well as the divergence of the interband polarization, are in general nonvanishing quantities, coupling the different polarization components of the optical field. However, if the semiconductor is initially in its ground state, for excitation with an ultrashort optical pulse with central frequency ω_L and spectral width $\Delta\omega$, we can choose the conditions such that the pulse resonantly excites only the lowest heavy-hole exciton transition. For this situation, the contribution from the light holes to the interaction Hamiltonian can be neglected. Furthermore, if the laser pulse propagates in the growth direction of a MQW, the interband polarization is homogeneous with respect to the in-plane coordinates and the macroscopic charge and current density vanish. Note that for perpendicular incidence, no center-of-mass motion of the electron-hole pair can be excited. Since the dipole matrix element for the heavy-hole transition has no z component, the wave equations for the different polarization components are decoupled by momentum conservation within the QW plane. For each σ^\pm polarization component the wave equation therefore simplifies to

$$\left(\frac{\partial^2}{\partial z^2} - \frac{1}{c^2} \frac{\partial^2}{\partial t^2}\right) E(z, t) = 4\pi \frac{1}{c^2} \frac{\partial^2}{\partial t^2} P(z, t). \quad (2)$$

Within the envelope function approximation,¹⁷ the z dependence of the macroscopic interband polarization is determined by the electron and hole confinement wave functions located at the positions z_n of the n th QW,

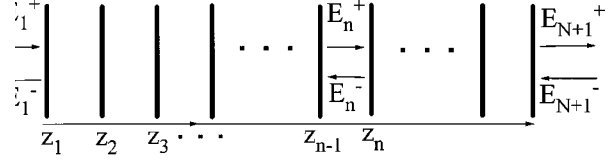


FIG. 1. Schematic illustration of the various counterpropagating wave packets in a MQW.

$$P(z, t) = \sum_n P^n(t) \varphi_e^n(z) \varphi_h^n(z) \approx \sum_n P^n(t) \delta(z - z_n). \quad (3)$$

Since Eq. (3) is used in the Maxwell equation (2), where the characteristic length scales are governed by the wavelength of light, we have approximated the product of the confinement wave functions by δ functions in Eq. (3). Denoting by k_L the wave vector of the light field, by L the width of the QW, and assuming perfect confinement of the electron and hole wave functions within the individual wells, the corrections to our equations due to the finite width of the QW are of the order $(k_L L)^2$, and can be neglected for appropriately chosen structures.

Formally, Eq. (2) can be solved without a detailed knowledge of the polarization by putting

$$E(z, t) = E_n^+ \left(t - \frac{z}{c}\right) + E_n^- \left(t + \frac{z}{c}\right) \quad (4)$$

in the n th barrier ($z_{n-1} < z < z_n$) as illustrated in Fig. 1 and applying the appropriate boundary conditions at the interfaces. Since the tangential components of the electric field are continuous at the interfaces, the first set of boundary conditions simply is

$$E_n^+ \left(t - \frac{z_n}{c}\right) + E_n^- \left(t + \frac{z_n}{c}\right) = E_{n+1}^+ \left(t - \frac{z_n}{c}\right) + E_{n+1}^- \left(t + \frac{z_n}{c}\right). \quad (5)$$

By integrating Eq. (2) from $z_n - \epsilon$ to $z_n + \epsilon$ and taking the limit $\epsilon \rightarrow 0$ we obtain as a second set of boundary conditions,

$$\left. \frac{\partial}{\partial z} \left[E_{n+1}^+ \left(t - \frac{z}{c}\right) + E_{n+1}^- \left(t + \frac{z}{c}\right) - E_n^+ \left(t - \frac{z}{c}\right) - E_n^- \left(t + \frac{z}{c}\right) \right] \right|_{z=z_n} = -\frac{1}{c} \frac{\partial}{\partial t} \left[E_{n+1}^+ \left(t - \frac{z_n}{c}\right) - E_{n+1}^- \left(t + \frac{z_n}{c}\right) - E_n^+ \left(t - \frac{z_n}{c}\right) + E_n^- \left(t + \frac{z_n}{c}\right) \right] = 4\pi \frac{1}{c^2} \frac{\partial^2}{\partial t^2} P^n(t). \quad (6)$$

Combining Eqs. (5) and (6) yields

$$E_n^+ \left(t - \frac{z}{c} \right) = E_1^+ \left(t - \frac{z}{c} \right) - 2\pi \sum_{m=1}^{n-1} \frac{1}{c} \frac{\partial}{\partial t} P^m \left(t - \frac{z-z_m}{c} \right), \quad (7a)$$

$$E_n^- \left(t + \frac{z}{c} \right) = E_{N+1}^- \left(t + \frac{z}{c} \right) - 2\pi \sum_{m=n}^N \frac{1}{c} \frac{\partial}{\partial t} P^m \left(t + \frac{z-z_m}{c} \right), \quad (7b)$$

where $E_1^+(t-z/c)$ and $E_{N+1}^-(t+z/c)$ are the external applied laser fields propagating in the positive and negative z directions, respectively.

To appreciate the direct consequences of Eqs. (7), it is instructive to discuss the single QW case at $z_1=0$ with the boundary conditions $E_1^+(t)=E_0(t)$ and $E_2^-(t)=0$. In this case, the transmitted field $E_2^+(t-z/c)$ equals the incident field $E_0(t-z/c)$ modified by the retarded time derivative of the polarization inside the QW. Simultaneously, the initial intensity is partly emitted in the backwards direction, i.e., reflected. The reflected field is identical to the modification of the transmitted field.

These considerations clearly show the importance of solving the full wave equation in an inhomogeneous structure. The often-used reduced wave equation, where second-order derivatives of the field envelopes are neglected, gives no back-propagating solutions. However, by dropping the back-propagating solutions of the full wave equation, the only consistent solution does not allow for any interaction at all, since in that case the transmitted field has to equal the incident field.

Apart from the external inputs the expressions for the total transmitted and reflected fields, E_{N+1}^+ and E_1^- , for a MQW appear to be very symmetric. Nevertheless, the temporal shape of E_{N+1}^+ and E_1^- can differ considerably as a consequence of the retarded time arguments. If we make the slowly varying envelope approximation (SVEA) in time,

$$E_n^\pm(t) = e^{-i\omega_L t} \tilde{E}_n^\pm(t), \quad (8a)$$

$$P^n(t) = e^{-i\omega_L t} \tilde{P}^n(t), \quad (8b)$$

Eqs. (7) can be simplified to

$$\tilde{E}_n^+(t) = \tilde{E}_1^+(t) + 2\pi i k_L \sum_{m=1}^{n-1} e^{-ik_L z_m} \tilde{P}^m(t), \quad (9a)$$

$$\tilde{E}_n^-(t) = \tilde{E}_{N+1}^-(t) + 2\pi i k_L \sum_{m=n}^N e^{ik_L z_m} \tilde{P}^m(t). \quad (9b)$$

In order to arrive at these expressions the retardation and the time derivative of the slowly varying envelope has been neglected. If \mathcal{L} is the thickness of the entire sample, this approximation corresponds to a coarse graining in time of the order of $\mathcal{L}/c \approx 1-10$ fs for typical semiconductor parameters. From Eqs. (9) it can be seen that apart from the external fields, the transmitted and reflected pulses are equal only if $\exp(ik_L z_m) = \exp(-ik_L z_m)$ for all m , i.e., in a structure

where the QW spacing is an integer multiple of a half wavelength. Otherwise, the retardation effects lead to interferences that cause an asymmetry between the transmitted and reflected pulses.

From Eqs. (7) we can compute the following observable quantities for a structure containing N quantum wells:

$$\alpha(\omega) = \frac{1}{N} \ln \left| \frac{E_0^+(\omega)}{E_{N+1}^+(\omega)} \right|^2, \quad (10a)$$

$$w(\omega) = \frac{1}{N} \frac{|E_0^+(\omega)|^2 - |E_{N+1}^+(\omega)|^2 - |E_1^-(\omega)|^2}{|E_0^+(\omega)|^2}. \quad (10b)$$

Here, we denote by $\alpha(\omega)$ the logarithm of the ratio of transmitted and input intensity, which in homogeneous media yields the absorption spectrum which is proportional to the imaginary part of the optical susceptibility.⁹ In order to avoid confusion we refer to this quantity as *transmission spectrum*, whereas the true absorption $w(\omega)$ is defined as that part of the intensity which remains inside the sample, i.e., is neither transmitted nor reflected. For a single QW, it can be shown that $w = -2 \operatorname{Re}(R^*T)$, where R is the reflection and T the transmission coefficient, thus showing that absorption, transmission, and reflection always occur simultaneously.¹⁴

Equations (7) and (10) are still quite general, since no other assumptions besides the dipole selection rules and the planar localization of the microscopic polarization have been made. Due to the QW coupling by the light field, both the transmission and the absorption spectrum in general depend on the number of QW's as well as on the sample geometry, as will be investigated in the next section.

B. The semiconductor Bloch equations for radiatively coupled quantum wells

For explicit model calculations of MQW's using the equations derived in the previous section, we compute the electronic polarization $P^n(t)$ from the SBE's. These equations have been shown to provide a good approximation to the optical response of pulse excited semiconductors.⁹ The coherent part of the electronic dynamics results from a Hartree-Fock approximation in the equations of motion derived from a two-band Hamiltonian and can be written as

$$\frac{\partial}{\partial t} \tilde{P}_{\mathbf{k}_\parallel}^n = -i(\omega_{\mathbf{k}_\parallel} - \omega_L) \tilde{P}_{\mathbf{k}_\parallel}^n - i(2n_{\mathbf{k}_\parallel}^n - 1) \tilde{\Omega}_{R, \mathbf{k}_\parallel}^n, \quad (11a)$$

$$\frac{\partial}{\partial t} n_{\mathbf{k}_\parallel}^n = -2\mathcal{I}(\tilde{\Omega}_{R, \mathbf{k}_\parallel}^n \tilde{P}_{\mathbf{k}_\parallel}^{n*}). \quad (11b)$$

Here $\tilde{P}_{\mathbf{k}_\parallel}^n$ is the polarization for a one-particle momentum state in the n th quantum well and $n_{\mathbf{k}_\parallel}^n$ is the carrier distribution function for the electrons and holes. The total macroscopic polarization entering Eqs. (1), (2), and (7) is obtained by summing over all different momentum states,

$$\tilde{P}^n(t) = \sum_{\mathbf{k}_\parallel} d_{c\nu} \tilde{P}_{\mathbf{k}_\parallel}^n(t), \quad (12)$$

where d_{cv} is the magnitude of the dipole matrix element. The renormalized single-particle energy $\omega_{\mathbf{k}_\parallel}$ and the local Rabi frequency $\tilde{\Omega}_{R,\mathbf{k}_\parallel}^n$ are given by

$$\omega_{\mathbf{k}_\parallel} = \bar{E}_g + \frac{\mathbf{k}_\parallel^2}{2m_r} - 2 \sum_{\mathbf{q}_\parallel \neq \mathbf{k}_\parallel} V_{\mathbf{k}_\parallel - \mathbf{q}_\parallel}^{nn} n_{\mathbf{q}_\parallel}^n, \quad (13a)$$

$$\begin{aligned} \tilde{\Omega}_{R,\mathbf{k}_\parallel}^n &= d_{cv} (e^{ik_L z_n} \tilde{E}_n^+ + e^{-ik_L z_n} \tilde{E}_n^-), \\ &+ \sum_{\mathbf{q}_\parallel \neq \mathbf{k}_\parallel} V_{\mathbf{q}_\parallel - \mathbf{k}_\parallel}^{nn} \tilde{P}_{\mathbf{q}_\parallel}^n. \end{aligned} \quad (13b)$$

Here, \bar{E}_g is the band-gap energy including the confinement energy and $V_{\mathbf{q}_\parallel}^{nm}$ is the two-dimensional Coulomb interaction acting between the n th and m th quantum wells. In the case of a vanishing two-particle interaction the SBE's reduce to the two-level Bloch equations.

In the two-dimensional (2D) approximation the bare Coulomb interaction is given by

$$V_{\mathbf{q}_\parallel}^{nm,2D} = \frac{2\pi}{A} \frac{1}{q_\parallel} e^{-q_\parallel |z_n - z_m|},$$

where A is the total area of the QW. Although this 2D limit is justified when dealing with light propagation effects where the relevant length scale is the wavelength of the exciting optical field [see Eq. (3)], the relevant length scale for treating the Coulomb interaction as two-dimensional is the excitonic Bohr radius. Since the width of a realistic QW is often of the same order of magnitude as the excitonic Bohr radius, we include the corrections due to the finite well width as

$$V_{\mathbf{q}_\parallel}^{nm} = V_{\mathbf{q}_\parallel}^{nm,2D} \zeta^{nm}(q_\parallel L), \quad (14)$$

with

$$\zeta^{nm}(q_\parallel L) = \frac{4}{L^2} \int_{-L/2}^{L/2} dz dz' \cos^2 \frac{\pi z}{L} \cos^2 \frac{\pi z'}{L} e^{-q_\parallel |z - z'|}, \quad (15)$$

$$\zeta^{nm}(q_\parallel L) = \left(\frac{2}{q_\parallel L} \sinh \frac{q_\parallel L}{2} \frac{1}{(q_\parallel L / 2\pi)^2 + 1} \right)^2 \text{ for } n \neq m, \quad (16)$$

where we have assumed infinitely high potential barriers.

Inserting the solution of Maxwell's equations (7) in the generalized Rabi frequency Eq. (13b) reduces the problem to

that of finding the solution of the SBE's with a self-consistently determined radiation field,

$$\begin{aligned} \tilde{\Omega}_{R,\mathbf{k}_\parallel}^n &= d_{cv} (e^{ik_L z_n} \tilde{E}_1^+ + e^{-ik_L z_n} \tilde{E}_{N+1}^-) \\ &+ 2\pi i k_L d_{cv}^2 \sum_{m=1}^N \sum_{\mathbf{q}_\parallel} e^{ik_L d_{mn}} \tilde{P}_{\mathbf{q}_\parallel}^m + \sum_{\mathbf{q}_\parallel \neq \mathbf{k}_\parallel} V_{\mathbf{q}_\parallel - \mathbf{k}_\parallel}^{nn} \tilde{P}_{\mathbf{q}_\parallel}^n, \end{aligned} \quad (17)$$

where d_{nm} is the distance between the n th and the m th QW. From this equation, one recognizes that the different QW's are coupled by a dynamical dipole-dipole interaction mediated by the exchange of transverse photons. Due to this dipole-dipole interaction, the dynamics of the electronic polarization not only depends on the total QW number, but via the phase factor $e^{ik_L d_{mn}}$ also on the spacing between the QW's.

The SMBE's can be simplified somewhat if we define

$$\tilde{P}^{n\pm} = e^{\pm ik_L z_n} \tilde{P}^n, \quad (18a)$$

$$\tilde{\Omega}^{n\pm} = e^{\pm ik_L z_n} \tilde{\Omega}^n, \quad (18b)$$

corresponding to plane waves propagating in the positive or negative z direction. Note that without the SVEA these quantities correspond to $P^n(t \pm z_n/c)$. Using the transformed quantities (18), the transmitted and reflected fields can be expressed as

$$\tilde{E}_{N+1}^+(t) = \tilde{E}_1^+(t) + 2\pi i k_L \sum_{n=1}^N P^{n+}(t), \quad (19a)$$

$$\tilde{E}_1^-(t) = \tilde{E}_{N+1}^-(t) + 2\pi i k_L \sum_{n=1}^N P^{n-}(t), \quad (19b)$$

respectively; see Eqs. (9). Thus, the transmitted (reflected) field depends on the polarization wave propagating in the forward (backward) direction only.

The SBE's can also be expressed in terms of either the forward or backward propagating waves, e.g.,

$$\frac{\partial}{\partial t} \tilde{P}_{\mathbf{k}_\parallel}^{n+} = -i(\omega_{\mathbf{k}_\parallel} - \omega_L) \tilde{P}_{\mathbf{k}_\parallel}^{n+} - i(2n_{\mathbf{k}_\parallel}^n - 1) \tilde{\Omega}_{R,\mathbf{k}_\parallel}^{n+}, \quad (20a)$$

$$\frac{\partial}{\partial t} n_{\mathbf{k}_\parallel}^n = -2\mathcal{J}(\tilde{\Omega}_{R,\mathbf{k}_\parallel}^{n+} \tilde{P}_{\mathbf{k}_\parallel}^{n+*}), \quad (20b)$$

with

$$\tilde{\Omega}_{R,\mathbf{k}_\parallel}^{n+} = d_{cv} (\tilde{E}_1^+ + e^{-2ik_L z_n} \tilde{E}_{N+1}^-) + 2\pi i k_L d_{cv}^2 \sum_{m=1}^n \sum_{\mathbf{q}_\parallel} \tilde{P}_{\mathbf{q}_\parallel}^{m+} + 2\pi i k_L d_{cv}^2 \sum_{m=n+1}^N \sum_{\mathbf{q}_\parallel} e^{2ik_L d_{mn}} \tilde{P}_{\mathbf{q}_\parallel}^{m+} + \sum_{\mathbf{q}_\parallel \neq \mathbf{k}_\parallel} V_{\mathbf{q}_\parallel - \mathbf{k}_\parallel}^{nn} \tilde{P}_{\mathbf{q}_\parallel}^{n+}. \quad (21)$$

From this set of equations, one recognizes that the observable quantities only depend on the phase shift accumulated while traveling backward *and* forward [$\exp(2ik_L d_{mn})$] rather than on the phase shift [$\exp(ik_L d_{mn})$] obtained by just traveling one way to the n th quantum well.

At this point, it should be noted that in the case of a finite in-plane photon momentum of the initial pulse, the polarization not only depends on the relative momentum but also on the total center-of-mass momentum $\mathbf{k}_{\parallel\text{com}}$ of the electron-hole pair. Due to the in-plane momentum conservation, the center-of-mass momentum can only be an integer multiple of the in-plane photon momentum $\mathbf{k}_{\parallel L}$. Neglecting charge separation due to the dispersive motion of the polarization and the carrier distribution functions, the long-ranged part of the interwell Coulomb interaction gives rise to an additional term in the generalized Rabi frequency (compare Ref. 18), that is obtained from the second term on the right-hand side of Eq. (17) by replacing k_L by $ik_{\parallel\text{com}}$ in the exponent and by $ik_{\parallel\text{com}}/2$ in the prefactor. The finite rangedness of this static dipole-dipole or Förster interaction, which is mediated by the exchange of longitudinal photons, is a direct consequence of the instantaneous character of the Coulomb interaction and results in a quite different geometry dependence than the dynamical, retarded dipole-dipole interaction derived in this paper. Moreover, due to the prefactor $k_{\parallel\text{com}}$, the Förster interaction vanishes exactly for perpendicularly incident light, and is usually small compared to propagation effects even if the initial pulse has a finite angle to the normal of the QW plane.

III. RESULTS AND DISCUSSION

To illustrate the basic features of our approach in this section, we evaluate the coupled equations assuming weak optical excitation. For this purpose, we expand the polarization in terms of the two-dimensional excitonic states φ_λ ($\lambda = \{n, m\}$ for bound states, $\lambda = \{k, m\}$ for continuum states),

$$\tilde{P}^n(t) = \sum_\lambda \gamma_\lambda \tilde{P}_\lambda^n(t), \quad (22)$$

which are the solutions of the Wannier equation.⁹ The expansion coefficients are determined by

$$\begin{aligned} \frac{\partial}{\partial t} \tilde{P}_\lambda^n(t) = & -i(\omega_\lambda - \omega_L) \tilde{P}_\lambda^n(t) + i\gamma_\lambda [e^{ik_L z_n} \tilde{E}_1^+(t) \\ & + e^{-ik_L z_n} \tilde{E}_{N+1}^-(t)] \\ & - \sum_{m\lambda'} \Gamma_{\lambda\lambda'} e^{ik_L d_{mn}} \tilde{P}_{\lambda'}^m(t). \end{aligned} \quad (23)$$

Here $\omega_\lambda = \bar{E}_g + \epsilon_\lambda$ is the effective band gap for the exciton state λ and $\gamma_\lambda = d_{cv} \varphi_\lambda(0)$ and $\Gamma_{\lambda\lambda'} = 2\pi k_L \gamma_\lambda \gamma_{\lambda'}$ are the radiative coupling strengths of the states λ . Within each QW, the nondiagonal part of the interaction with the induced field couples different excitonic states, whereas the diagonal part causes a radiative damping with a damping constant proportional to the oscillator strength of the corresponding state. These effects are comparable with the effects of a weak disorder due to interface roughness^{14,16} and clearly demonstrate

the fact that each excitonic transition interacts with photons emitted from all other transitions. Furthermore, through the phase factors $\exp(ik_L d_{mn})$, propagation effects couple the different QW's depending on the geometry of the structure.

In the frequency domain, Eq. (23) can be solved by matrix inversion, yielding

$$\begin{aligned} \tilde{P}^n(\omega) = & d_{cv} \tilde{E}_1^+(\omega) \sum_m \chi^{nm}(\omega) e^{ik_L z_m} \\ & + d_{cv} \tilde{E}_{N+1}^-(\omega) \sum_m \chi^{nm}(\omega) e^{-ik_L z_m}, \end{aligned} \quad (24)$$

where

$$\chi^{nm}(\omega) = \sum_{\lambda\lambda'} \gamma_\lambda \chi_{\lambda\lambda'}^{nm}(\omega) \gamma_{\lambda'}. \quad (25)$$

It is interesting to investigate the pole structure of the so-defined linear susceptibility, since the poles correspond to resonances of the coupled exciton radiation system. These resonances can be interpreted as quasiparticles in analogy to exciton polaritons in bulk semiconductors. The poles are obtained by solving

$$|(\omega - \omega_\lambda + \omega_L + i\Gamma_\lambda) \delta_{\lambda\lambda'}^{nm} + i\Gamma_{\lambda\lambda'} e^{ik_L d_{nm}} (1 - \delta_{\lambda\lambda'}^{nm})| = 0.$$

While in a bulk material the pole structure of the linear susceptibility yields the polariton dispersion relation, the MQW susceptibility has N discrete (eventually degenerate) poles that are in general complex since the matrix is non-Hermitian. The real parts of the solutions correspond to the energy of the quasiparticles, whereas the imaginary parts correspond to a radiative broadening of the resonances. Note that due to the summation over the QW indices in Eqs. (7) and (24) not all resonances necessarily contribute to the transmitted or reflected signal. Some resonances may correspond to ‘‘dark’’ solutions that are not observable in far-field optical spectroscopy.

An interesting situation arises if the QW spacing is an integer multiple of $\lambda/2$. Both in transmission and reflection geometry, $\sum_n (-1)^n \tilde{P}^n$ is observed, which is an eigenvector with eigenvalue N of the matrix $\mathcal{D}_{mn} = \exp(ik_L d_{mn}) = (-1)^{n+m}$ that determines the geometrical part of the inverse susceptibility. Hence, the radiative coupling strengths and linewidths of the excitonic states that contribute to the *observable* fields increase linearly with the QW number. All other eigenvectors have the eigenvalue 0, thus having a vanishing radiative coupling and linewidth. Exactly for this reason, these resonances *cannot be optically excited at all*, making them invisible not only for detection by far-field optical spectroscopy but also in optical near-field microscopy that allows us in principle to analyze contributions from the individual QW. This type of coupling leads to a so-called superradiant state with a fast stimulated decay of electronic excitations, as shown in Fig. 2(a) for the case of two QW's. As the QW's are excited simultaneously with an intensity maximum of the laser pulse, the excited exciton density will be more or less equally distributed among the structure (small deviations can arise from the asymmetry in the initial conditions in a single pulse configuration). A photon emitted in a spontaneous recombination process of the electron-hole

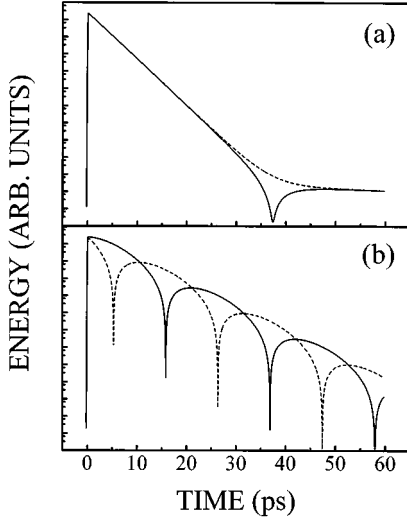


FIG. 2. Time-resolved excitation energy in the first QW (solid line) and the second QW (dashed line) of a double QW located at a distance of half a wavelength (a) and a quarter wavelength (b).

pair in any given QW can either give rise to a stimulated decay or can be reabsorbed. However, reabsorption is a second-order process and of minor importance at low optical excitation, so that the stimulated decay processes dominate.

Another interesting case is realized if $\exp(ik_L d_{nm})$ is purely imaginary for all $m \neq n$. This situation can be realized in a double QW structure with $z_1 - z_2 = (2n + 1)\lambda/4$, where λ is the wavelength of the laser pulse. Then the interwell coupling leads to a pure splitting of resonances. In a $\lambda/4$ structure, the coupling leads to an oscillatory energy transfer from one quantum well to the other; see Fig. 2(b). At a given time the light intensity has a maximum at the position of the first QW and the second QW is located in an intensity minimum and vice versa at a different time. Hence, an emitted photon interacts with a nonexcited neighboring QW, where the only possible interaction mechanism is reabsorption which is now a first-order process. Qualitatively, this behavior equals the dynamics of two coupled harmonic oscillators, where one of the oscillators is initially excited, whereas the second initially is in its ground state.

In Fig. 3, we plot the linear transmission spectra $\alpha(\omega)$ calculated in the vicinity of the $1s$ -hh excitonic resonance¹⁹ for a $\lambda/2$ and a $\lambda/4$ structure containing one, two, and ten QW's. One clearly recognizes the dependence on the total number of wells as well as on the barrier thickness, even though the barriers are optically inactive. The (normalized) transmission in the $\lambda/2$ structure decreases significantly with the QW number, whereas the transmission spectrum of a $\lambda/4$ structure is much less sensitive to the total number of quantum wells. Note that although the transmission line shapes are clearly non-Lorentzian, the level splitting occurring in the pole structure of the linear susceptibility can hardly be observed. This changes dramatically if one looks at the true absorption, as defined in Eq. (10b).

Figure 4 shows the absorption spectra for the same parameters used in Fig. 3. The true absorption exhibits a very rich fine structure for a MQW structure, depending sensitively on the structure periodicity. For the $\lambda/2$ structure, the absorption decrease per QW is even more pronounced than

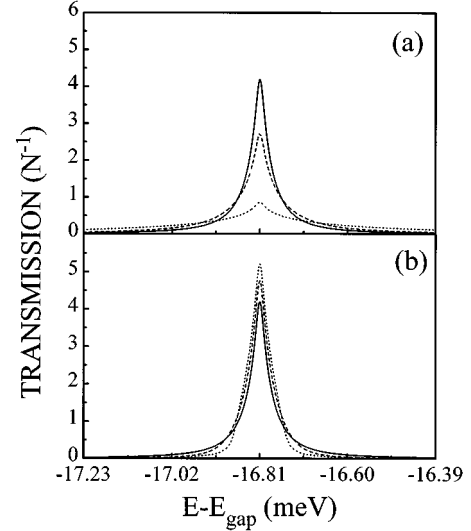


FIG. 3. Normalized transmission spectra for one (solid line), two (dashed line), and ten (dotted line) MQW's in a $\lambda/2$ (a) and a $\lambda/4$ (b) structure. The spectra have been normalized to the total number of quantum wells N .

the transmission decrease. The lack of fine structure is a consequence of the fact that only one mode is optically accessible, having a radiative linewidth N times enhanced compared to the case of a single QW. On the other hand, the level splitting in a $\lambda/4$ structure is clearly observable in its true absorption spectrum, having two maxima for the double QW sample and a substantial number of less pronounced maxima for a MQW. By inserting the linear interband polarization on the right hand side of Eq. (11b) one finds that the true absorption is proportional to the total number of excited electron-hole pairs

$$N_{e/h} = \sum_{n\mathbf{k}_{\parallel}} n_{\mathbf{k}_{\parallel}}^n(t \rightarrow \infty) \propto \int \frac{d\omega}{2\pi} w(\omega) |\tilde{E}_1^+(\omega)|^2, \quad (26)$$

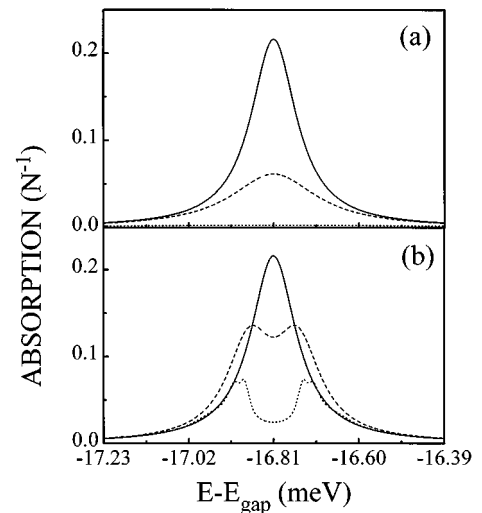


FIG. 4. Normalized absorption spectra for one (solid line), two (dashed line), and ten (dotted line) MQW's in a $\lambda/2$ (a) and a $\lambda/4$ (b) structure.

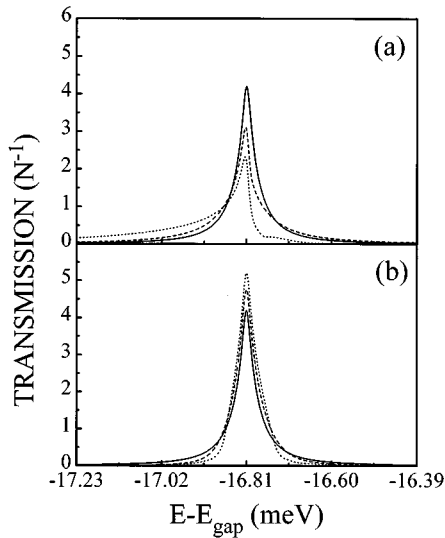


FIG. 5. As in Fig. 3 but for a structure where the distance between the QW's is 2 nm less than $\lambda/2$ (a) or $\lambda/4$ (b).

and should thus be observable, e.g., by time-integrated excitation luminescence spectroscopy.

To demonstrate the extraordinary sensitivity of the results on the spacing between the quantum wells, we show in Figs. 5 and 6 the calculated transmission and absorption spectra for a structure with one, two, and ten QW's with a period slightly less than $\lambda/2$ or $\lambda/4$ ($\Delta D = -2nm$). Comparing Figs. 3 and 4 with Figs. 5 and 6, we notice dramatic changes of the spectra, especially substantial modifications of the absorption for the small variation of the barrier thickness. In particular, a small deviation from the $\lambda/2$ periodicity gives rise to a nonzero coupling to modes having a very small radiative linewidth that are optically forbidden if the spacing is exactly $\lambda/2$. Since these modes dominate the long-time behavior of electronic excitations, this observation is of crucial importance for a correct interpretation of time-resolved

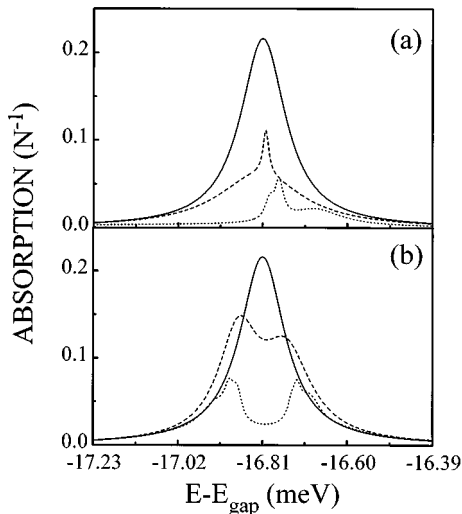


FIG. 6. As in Fig. 4 but for a structure where the distance between the QW's is 2 nm less than $\lambda/2$ (a) or $\lambda/4$ (b).

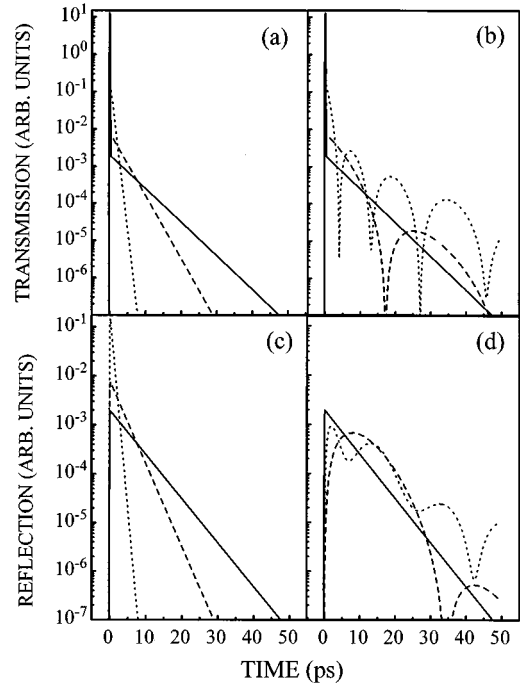


FIG. 7. Time-resolved transmission spectra for one (solid line), two (dashed line), and ten (dotted line) MQW's in a $\lambda/2$ (a) and a $\lambda/4$ (b) structure. (c) and (d) show the reflected intensities.

measurements on samples containing a large number of QW's positioned at approximately $\lambda/2$.

In Fig. 7 we show computed examples of the linear time-resolved transmission and reflection for perfect $\lambda/2$ and $\lambda/4$ structures. We assume resonant 1s exciton excitation with a 100-fs pulse full width at half maximum. A comparison of Figs. 7(a) and 7(c) demonstrates that for the $\lambda/2$ structure reflection and transmission are identical for times after the exciting pulse has decayed. Furthermore, the decay rate in-

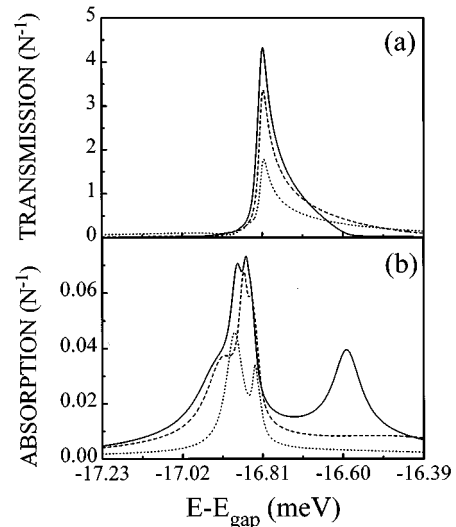


FIG. 8. Normalized transmission (a) and absorption (b) spectra for ten MQW's with a total length of λ (solid line), $\lambda/2$ (dashed line), and $\lambda/10$ (dotted line).

creases linearly with N (to be precise, $1/T_2 = \gamma_0 + N\gamma_{\text{rad}}$, where γ_0 is the nonradiative homogeneous linewidth). For a $\lambda/4$ structure, the transmitted and reflected signals exhibit quantum beats, which is the time-domain signature of the splitting of the absorption peaks; see Fig. 4. Furthermore, the transmitted and reflected signals display pronounced differences due to interference effects.

To study the length dependence of the optical response, we plot in Fig. 8 the normalized transmission and absorption spectra for a system of ten quantum wells with a total length of λ , $\lambda/2$, and $\lambda/10$. We notice a gradual decrease of transmission with decreasing sample length. Also the asymmetry of the absorption spectrum decreases somewhat, but the overall features show clearly, that even for barrier thicknesses much less than the optical wavelength, multiple reflections dominate the optical spectra.

IV. CONCLUSIONS

In conclusion, we presented the semiconductor Maxwell-Bloch equations for an optical pulse interacting with a semiconductor multiple-quantum-well structure. We have shown that the propagation-induced dynamical dipole-dipole interaction leads to a coupling of electronic excitations in different quantum wells, resulting in a collective behavior of the electronic dynamics. Contrary to electronic coupling such as

tunneling, the light-induced coupling does not necessarily lead to a splitting of resonances, but can also result in a pure broadening of excitonic linewidths.

The origin of these phenomena is the phase coherence of the electronic excitations that is determined by the spacing between the QW's. Comparing the QW excitons with a string of localized oscillators, the radiative coupling causes a stimulated emission of photons if the oscillators are all in phase ($\lambda/2$ MQW), whereas an oscillatory energy transfer can occur if they are exactly out of phase ($\lambda/4$ MQW). Our calculations indeed predict this behavior. For all geometries, the radiative coupling induces a memory into the system, since the polarization in the n th QW is coupled to the retarded time derivative of the polarization in all distinct QW's. For this reason, a more or less pronounced increase of the decay time with increasing QW number can be observed. We expect that the broadening and splitting of excitonic resonances found in the linear spectra will also manifest themselves in nonlinear experiments, such as four-wave mixing experiments.

ACKNOWLEDGMENT

This work has been supported by the Deutsche Forschungsgemeinschaft, partially through the Sonderforschungsbereich 383.

-
- ¹See, e.g., *Optics of Excitons in Confined Systems*, edited by G. Bastard and B. Gil [J. Phys. (France) IV 3 (1993)].
- ²D. Weber, J. Feldmann, T. Stroucken, A. Knorr, S.W. Koch, D.S. Citrin, K. Köhler, and E.O. Göbel, J. Opt. Soc. Am. B (to be published).
- ³P.A. Harten, A. Knorr, J.P. Sokoloff, F. Brown de Colstoun, S.G. Lee, R. Jin, E.M. Wright, G. Khitrova, H.M. Gibbs, S.W. Koch, and N. Peyghambarian, Phys. Rev. Lett. **69**, 852 (1992).
- ⁴S.W. Koch, A. Knorr, R. Binder, and M. Lindberg, Phys. Status Solidi B **173**, 177 (1992)
- ⁵J. Aaviksoo, J. Kuhl, and K. Ploog, Phys. Rev. A **44**, R5353 (1991).
- ⁶T. Mishina and Y. Masumoto, Phys. Rev. Lett. **71**, 2785 (1993).
- ⁷R. Laenen and A. Laubereau, Opt. Commun. **101**, 43 (1993).
- ⁸D. Fröhlich, A. Kulik, B. Uebbing, A. Myssyrowicz, V. Langer, H. Stolz, and W. von der Osten, Phys. Rev. Lett. **67**, 2343 (1991).
- ⁹See, e.g., H. Haug and S.W. Koch, *Quantum Theory of the Optical and Electronic Properties of Semiconductors*, 3rd ed. (World Scientific, Singapore, 1994), and references therein.
- ¹⁰See, e.g., L.C. Andreani, in *Confined Electrons and Photons: New Physics and Devices*, edited by C. Weisbuch (Plenum, New York, 1995), and references therein.
- ¹¹D.S. Citrin, in *Confined Electrons and Photons: New Physics and Devices* (Ref. 10).
- ¹²Y. Chen *et al.*, Europhys. Lett. **14**, 483 (1991).
- ¹³G. Manzke and K. Henneberger, Phys. Status Solidi B **147**, 733 (1988).
- ¹⁴T. Stroucken, A. Knorr, C. Anthony, A. Schulze, P. Thomas, S.W. Koch, M. Koch, S.T. Cundiff, J. Feldmann, and E.O. Göbel, Phys. Rev. Lett. **74**, 2391 (1995)
- ¹⁵A. Knorr, T. Stroucken, A. Schulze, A. Girndt, and S.W. Koch, Phys. Status Solidi B **188**, 473 (1995).
- ¹⁶T. Stroucken, C. Anthony, A. Knorr, P. Thomas, and S.W. Koch, Phys. Status Solidi B **188**, 539 (1995).
- ¹⁷G. Bastard, *Wave Mechanics Applied to Semiconductor Heterostructures* (Les Editions de Physique, Paris, 1988).
- ¹⁸M. Batsch, T. Meier, P. Thomas, M. Lindberg, S.W. Koch, and J. Shah, Phys. Rev. B **48**, 11 817 (1993).
- ¹⁹All parameters correspond to GaAs: $\Delta_{\text{LT}}=0.08$ meV, $\epsilon_0=12.9$, $1 \text{ Ry}=4.2$ meV, $E_{\text{gap}}=1.52$ eV. The radiative linewidth of the $1s$ exciton is given by $\gamma_{\text{rad}}(\omega)=0.25\Delta_{\text{LT}}\hbar\omega/c|\varphi_{1s}^{2d}(0)|^2/|\varphi_{1s}^{3d}(0)|^2$. At resonance, $\gamma_{\text{rad}}=0.048$ meV. For our calculations we use a homogeneous nonradiative linewidth of $\gamma_0=0.008$ meV, which is sufficiently small compared to the radiative linewidth to allow us to see the effects caused by the radiative coupling.